# A LOCALLY DEVELOPED 40 m$^2$ HELIOSTAT ARRAY WIRELESS CONTROL SYSTEM

## Karel J. Malan[1], Paul Gauché[2]

[1] Research Engineer STERG, Dept. Mechanical and Mechatronic Engineering, Stellenbosch University, Private Bag X1, Matieland, 7602. Phone: +27 21 808 4226, E-mail: karel@sun.ac.za

[2] Senior Researcher and Director STERG, Dept. Mechanical and Mechatronic Engineering, Stellenbosch University.

## Abstract

The ability of concentrating solar power (CSP) to efficiently store thermal energy sets it apart from other renewable energy technologies. The high initial cost of CSP limits its widespread deployment. Significant cost reduction opportunities exist, especially for central receiver systems (CRS) where the heliostat field typically makes up 40-50% of total cost.

CRS plants require heliostats with very high tracking accuracy. However, tracking errors occur due to manufacturing-, installation- and alignment tolerances as well as control system resolution. Typical heliostat tracking errors vary over the course of days and seasons and cannot be corrected by simple angle offsets. The objective of this research was to develop a wireless control system for Helio40, a 40m$^2$ heliostat array deployed on the STERG rooftop laboratory. A model based open-loop error correction method was used to minimize deterministic tracking errors over time. Individual heliostats' daily tracking error offsets were obtained periodically using a camera, calibration target and image processing techniques. Mathematical optimization was used to estimate error coefficients that best fit the measured curve. Real time error corrections were calculated for each heliostat by implementing the error model's rotation and translation operations in reverse order and applying three adjustment coefficients to the elevation linear actuator geometry. Initial tracking results obtained with a Helio40 heliostat showed an improvement of more than a full order of magnitude in the daily open-loop RMS tracking error.

*Keywords: Heliostat, Control System, Wireless.*

## 1. Introduction

One of the biggest barriers to large scale CSP deployment is its high initial cost compared to that of conventional power plants. However, CRS technology is still relatively immature, so it is widely considered to present the best opportunity for cost reduction (in utility scale deployment) of all CSP types [1]. The SunShot Initiative is a funding program launched in 2011 by the United States Department of Energy which aims to reduce the levelised cost of electricity [2] of CSP from its 2011 level of 15 ¢/kWh to under 6 ¢/kWh by 2020 [3]. Specific technology improvement opportunities (TIO) were identified to reduce the cost of the heliostat field, which typically makes up 40-50 per cent of a CRS plant's total cost [4],[5]. These TIO range from optimization of heliostat structures and drivetrains to improvements in tracking accuracy and communication networks, including:

- "Reliable wireless methods for heliostat power and communication.
- Advanced, self-aligning control systems." [1].

Looking closer to home, opportunities for job creation exist in South Africa if a local CSP industry can be developed to meet future domestic demand and eventually supply to the international market. At the time of writing, 200 MWe of CSP projects have already been awarded to major international players Abengoa and ACWA Power International under the Renewable Energy Independent Power Producer Procurement (REIPPP) program [6]. Significant opportunities exist due to increasing local content requirements in future REIPPP bidding rounds [7].

The aim of this paper is to report on the development of Helio40, a 40 m$^2$ heliostat array installed on the

Solar Thermal Energy Research Group (STERG) rooftop laboratory at Stellenbosch University.

## 2. Objective

The paper's specific focus is on the control system that governs the real time tracking and safety aspects of the Helio40 heliostats field. Various aspects of the control system architecture and individual components are discussed in the following sections. Finally, we present and discuss tracking results obtained by a Helio40 heliostat during on-sun tracking tests performed at the STERG rooftop laboratory.

## 3. Control method

### 3.1 Concept of operation

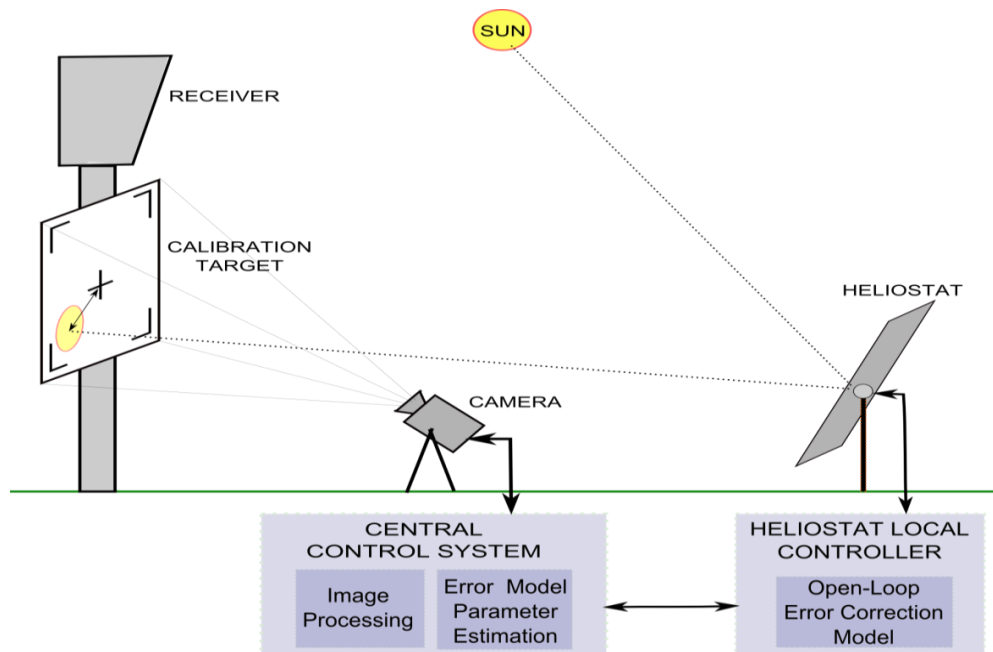The heliostat field array's main components are shown in Figure 1.



**Figure 1. Heliostat field components and error measurement concept of operation.**

Every heliostat in the system is periodically commanded to aim its reflected solar image at a calibration target separate from the receiver. A camera located in the field photographs the solar image projected onto the target and transfers the digital image to a central computer. Image processing techniques are used to calculate a time-stamped set of aim point offsets for each heliostat, as per Figure 2.
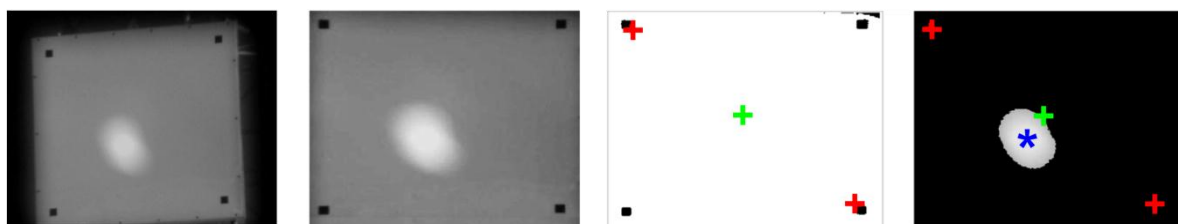


**Figure 2. Image processing sequence to calculate heliostat image centroid**

Due to the large number of heliostats in typical CRS plants, it can take several weeks to obtain calibration measurements for an entire array. This means that corrections applied to a heliostat should remain valid at

least until the next set of measurements can be taken.

### 3.2. Open-loop tracking

Commercial CRS plants make use of solar position algorithms as part of their heliostat tracking strategies [8]. Advances in microprocessor technology and the availability of highly accurate solar position algorithms provide accuracy, flexibility and repeatability at relatively low cost.

The Helio40 system makes use of an open source algorithm by Grena [9] to calculate the solar vector at each control interval. The algorithm was chosen for its low computational cost as compared to that of NREL [10], making it ideally suited to low cost embedded systems. Every heliostat's ideal normal vector is calculated analytically [11] by its local controller unit. Real time tracking error corrections are calculated and actuator control signals are generated based on the error corrected normal vector.

### 3.3. Heliostat model and real time correction

Derivation of an azimuth-elevation heliostat error model with eight error coefficients are shown in [12]. These error parameters are briefly discussed below:

- Pedestal tilt angles ($\varepsilon_{ptN}$) and ($\varepsilon_{ptE}$) describe the heliostat pylon's misalignment relative to true vertical.
- Bias angles ($\gamma_{bias}$) and ($\alpha_{bias}$) describe the azimuth- and elevation axes' reference offsets relative to true north and true horizontal, respectively.
- A non-orthogonality angle ($\varepsilon_{NO}$) describes the secondary axis' rotation relative to its ideal orientation orthogonal to the primary axis.
- Translations ($\Delta_Z$), ($\Delta_E$) and ($\Delta_N$) describe the heliostat's location offset away from its nominal coordinates in the upward-, eastward-, and northward directions, respectively.

Three additional coefficients ($\Delta_{LAa}$, $\Delta_{LAb}$ and $\Delta_{LAc}$) are added to handle the Helio40 heliostats' nonlinear elevation angle deviation due to manufacturing and assembly tolerances of the secondary axis linear actuator (LA). This angle deviation is expressed using triangular geometry and the cosine rule to minimize the number of error coefficients required, as per [13]. A step-wise representation of the current heliostat error model (azimuth-elevation with linear actuator driving the elevation axis) is shown in Figure 3.
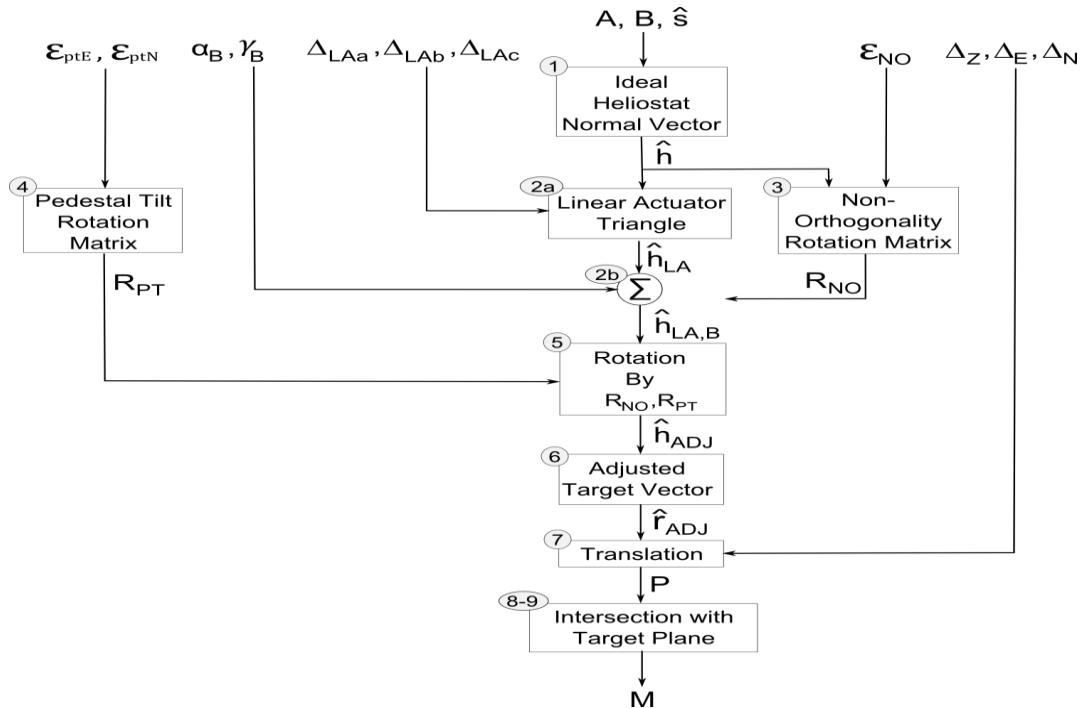


**Figure 3. Error model steps for azimuth-elevation heliostat with LA elevation axis.**

This sequence of transformations is reversed during real time error compensation calculations performed by the local controller of each heliostat.

## 4. Control system implementation

### 4.1 Distributed control architecture

Recent trends in CRS control systems show decentralization of low level tasks, largely due to the low cost and flexibility of modern microcontrollers (Camacho *et al.,* 2012:247). A distributed processing strategy was used for the Helio40 system whereby some tasks were centralized and others localized to each heliostat. Distributed processing allows the use of simple, low cost microcontrollers in the heliostat local controller units (LCUs). This may be an important driver for cost reduction since the ratio of LCUs to heliostats is inherently one-to-one.

The three processing tiers and high level dataflow are shown in Figure 4. Arrows indicate the flow of information up and down the processing hierarchy.
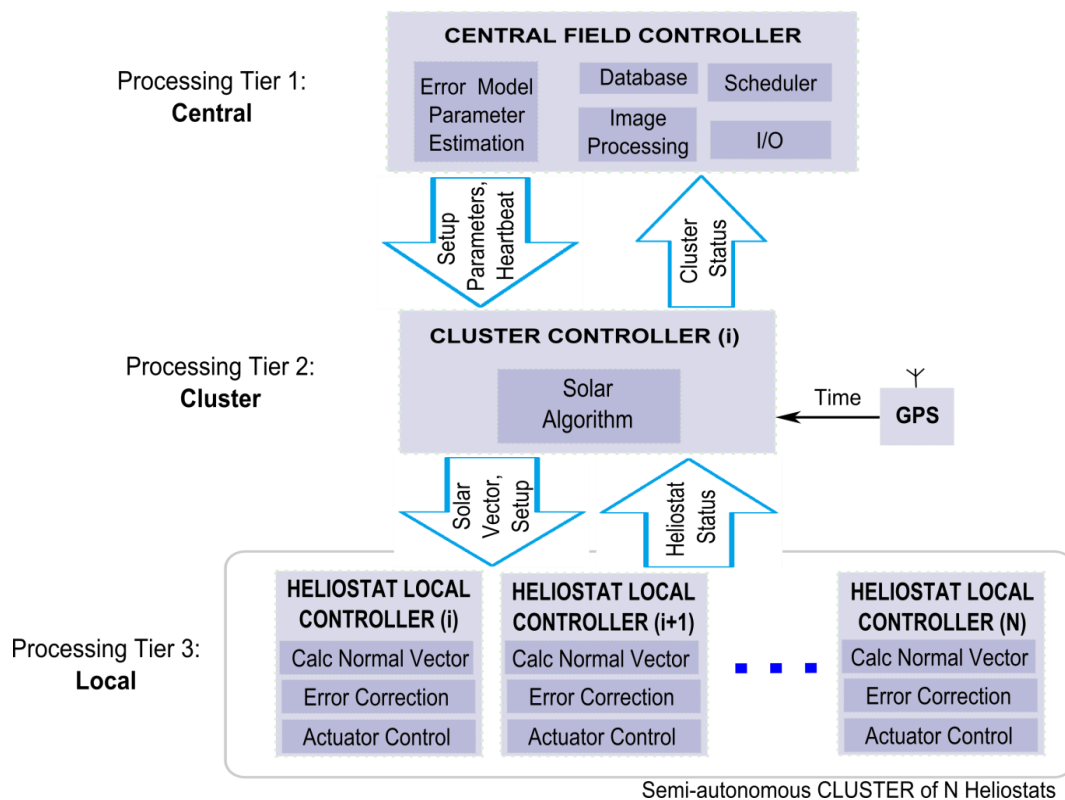


**Figure 4. Three-tiered distributed processing strategy**

### 4.2. Heliostat local control

Heliostat LCU boards were developed and tested over several months. Figure 5 shows a photograph of a prototype board featuring DC motor drivers, microcontroller (uC), actuator feedback signal conditioning and a digital radio transceiver module (RF TRX). The LCU boards currently use through-hole components for the motor driver ICs, the microcontroller chip and RF TRX to allow easy interchangeability for testing and validation purposes. Future development will focus on reducing cost and increasing efficiency. A transition to surface mount components may enable machine assembly.
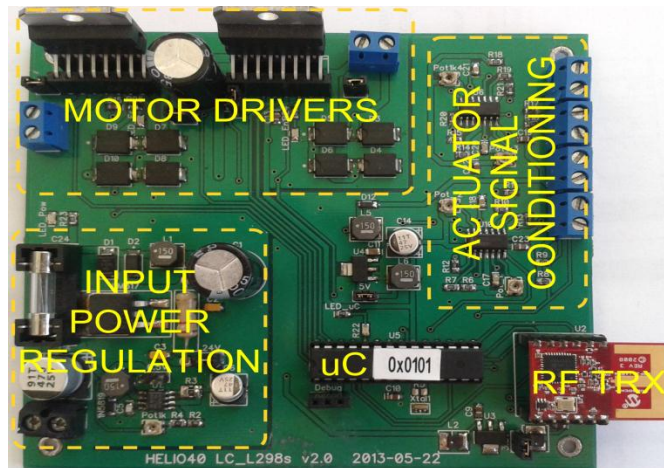
**Figure 5. Heliostat local controller board (v2.0).**

## 4.3. Cluster controller

Each cluster controller unit (CCU) calculates the solar position vector in real time and acts as communications multiplexer between the CCU and the cluster of heliostats under its control. It continuously monitors three communication channels:

1. The central controller PC sends configuration updates and queries to each CCU to adjust or query current system status or adjust individual heliostat parameter. After each tracking control interval, each CCU reports the status and step counts of all heliostats in its cluster to the central controller PC.

2. The GPS receiver transmits NMEA text strings at one second intervals. These strings are parsed to extract the current time and date for calculating the sun's angle using a solar position algorithm [9].

3. At the start of each control interval, the real-time calculated solar position is globally transmitted from the CCU to all heliostats in the cluster. Each heliostat in the cluster replies with its status and current step counts during predetermined communication time slots, assigned based on each unit's unique network address. The globally transmitted solar angles message is used by each LCU as timing reference for local timing of the communication slots.

## 4.4. Central controller

The central controller performs a number of predominantly non real-time tasks, including processing of tracking measurements, estimation of coefficients for the error model and a number of system monitoring-, calibration scheduling- and operator driven monitoring tasks via a graphical user interface.

## 4.5. Wireless communication and power

For multiple heliostats to function as an integrated solar concentrator, a communication network is required to reliably send and receive information between devices. A simple, custom data protocol was defined to standardise the way data is transmitted and received by all nodes in the network. To limit message size, a short packet structure was proposed, based loosely on the MODBUS protocol (modbus.org, 2012). At a minimum each packet contains 20 bytes:

- Message type (one byte allows up to 256 message types)
- Timestamp (two bytes for hour, minute, second information).
- Data payload (six bytes to contain high resolution solar angles, actuator counts or various status data)
- 11 bytes of medium access control (MAC) overhead, including:
  - Receiver address (two bytes allows up to $2^{16} = 65536$ unique addresses)
  - Destination address (two bytes)

- o   Cyclic redundancy code (two bytes)
- o   Five bytes containing frame information including packet length and signal quality metrics.

Microchip MRF24J40 wireless radio modules were used to for communicating between the heliostat local controllers and cluster controllers. These modules operate in the 2.45 GHz ISM band and allow up to 16 non-overlapping frequency channels to communicate at up to 250 kbps. By using a combination of time- and frequency division multiple access (TDMA / FDMA) for channel arbitration, up to 625 packets can be transmitted per second on each of the 16 available channels (including a rather conservative 50% dead time ratio), so up to 10 000 nodes could theoretically be controlled using this network layout and hardware. Bench testing of ten LCUs on a single channel confirmed the TDMA time-slotting assumptions stated above.

Power consumption of the current prototype boards is approximately 4 W per heliostat during normal tracking operation, so multiple heliostats could be connected to a single small (40 – 100 W) PV-and-battery 'island'. More detailed analysis of current consumption will be done with optimization of power consumption and increased power monitoring capabilities planned for the next generation of LCU boards.

## 5. Results and discussion

Daily tracking results are shown in Figure 6. The pre-calibration measurement set's heliostat normal vector RMS error was 27 mrad. Applying the calibration coefficients improved this error to 2.05 mrad, thus improving tracking performance by more than a full order of magnitude. Further improvements should be possible and ongoing research is directed at improving the heliostat error model and better understanding the parameter dependencies.
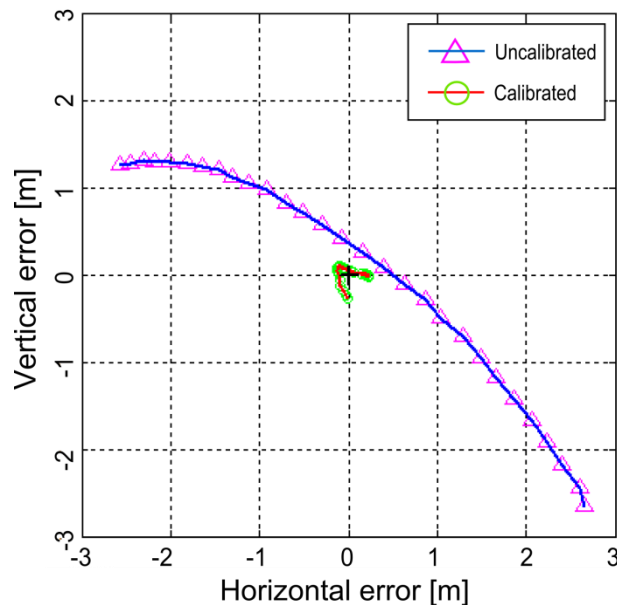


**Figure 6. Daily vertical- and horizontal tracking errors before and after calibration.**

## 6. Conclusion

This article presented the heliostat array control system used by Helio40. The system's wireless communication and power supply may allow cost reduction in larger systems by greatly reducing overall field wiring requirements and installation time. Further development is needed to minimize power consumption and to confirm modularity and communication reliability in larger systems. Tracking results presented here show that a model based method of open loop tracking and error correction may be an

appropriate solution for minimizing tracking errors since accurate results are obtainable using low tolerance heliostat mechanisms.

## Acknowledgements

## References

[1] Kolb, G. J., Ho, C. K., Mancini, T. R., Gary, J. A. 2011. Power Tower Technology Roadmap and Cost Reduction Plan. Sandia National Laboratories. [SAND2011-2419].

[2] International Renewable Energy Agency. 2012. *Renewable Energy Technologies: Cost Analysis of Concentrating Solar Power.* IRENA Working Paper.

[3] United States Department of Energy. 2011a. *DOE Pursues SunShot Initiative to Achieve Cost Competitive Solar Energy by 2020* [Online].
http://www1.eere.energy.gov/solar/sunshot/news_detail.html?news_id=16701. [2011, December 15].

[4] Ortega, J., Burgaleta, J., Téllez, F. 2008. Central Receiver System Solar Power Plant Using Molten Salt as Heat Transfer Fluid. *Journal of Solar Energy Engineering*, May 2008, Vol130 / 024501-1.

[5] Kolb, G. J., Jones, S. A., Donnelly, M. W., Gorman, D., Thomas, R., Davenport, R., Lumia, R. 2007. Heliostat Cost Reduction Study. Sandia National Laboratories, Albuquerque. [SAND2007-3293].

[6] CSP World. [S.a.]. *South Africa has allocated 200 MW of CSP in third round of REIPPP*. [Online]. http://www.csp-world.com/news/20130620/001089/south-africa-allocated-200-mw-csp-third-round-reippp.dpuf. [2013, October 28].

[7] Department of Trade and Industry of the Republic of South Africa. *Solar and Wind Sector Development Strategy: Solar Energy Technology Roadmap 18 June 2012.*

[8] Camacho, E. F., Berenguel, M., Rubio, F. R., Martìnez, D. 2012. *Advances in Industrial Control: Control of Solar Energy Systems*. Springer.

[9] Grena, R. 2007. *An Algorithm for the Computation of the Solar Position*. Solar Energy 82 462–470. ScienceDirect.

[10] Reda, I., Andreas, A. 2008. Solar Position Algorithm for Solar Radiation Applications. NREL/TP-560-34302.

[11] Stine, W. B., Geyer, M. 2001. *Power from the Sun*. [Online]. www.powerfromthesun.net.

[12] Malan, K. J., Gauché, P. 2013b. Model Based Open Loop Correction of Heliostat Tracking Errors. In: *SolarPACES 2013*. Las Vegas.

[13] Burton, A. I. Heliostat Calibration and Control. Patent Application WO2012083383 A1.